UNITED NATIONS UNIVERSITY
UNU-GTP
Geothermal Training Programme

Orkustofnun, Grensasvegur 9,
IS-108 Reykjavik, Iceland

Reports 2016
Number 23

ELECTROMAGNETIC EXPLORATION OF THE EYJAFJÖRDUR LOW-TEMPERATURE GEOTHERMAL AREA, N-ICELAND

András Kovács
Eötvös Lóránd University
Tolnay Károly str. 3
1163 Budapest
HUNGARY
bandee.k@gmail.com

ABSTRACT

This report discusses a resistivity survey, which was carried out in North Iceland, within the southern part of Eyjafjördur in 2012 and 2013 by Iceland GeoSurvey, ÍSOR. The dataset consists of TEM and MT measurements from the area, which are processed, 1D inverted and discussed. The methodology is shown, from data acquisition to the resulting resistivity model. In this study the relationship between the present work and former studies is discussed. Furthermore, a possible interpretation is evaluated on an enigmatic deep-seated resistivity anomaly, based on older magnetotelluric measurements as well as, recent structural geological and tectonic studies.

1. INTRODUCTION

Iceland's second most inhabited region is the Eyjafjördur area, where approximately twenty thousand people live and where one of the biggest city in the country, Akureyri is located. Around the fjord, six independent district heating systems serve the local municipalities. The most remarkable supplier is the Nordurorka, which owns four of these systems and operates around Akureyri. During the second part of the 20th century the increasing demand for hot water usage in the district heating system required new reservoir discoveries. In order to achieve reasonable success, DC resistivity soundings were carried out in the mid-seventies. As a result of this exploration a low-resistivity anomaly was found towards the south end of the fjord at the field Laugaland. This field was drilled into in 1975 and resulted in around 100 L/s of free flowing 96°C hot water. Another huge discovery was made in the early years of the 21st century, on the western coast of the fjord and north of Akureyri. A significant thermal anomaly was recognized in the vicinity of the village of Hjalteyri, which resulted in the discovery of a reservoir capable of serving 200 L/s of hot water (Flóvenz et al., 2010). In order to create realistic conceptual models and detailed numerical models, an improved picture of the reservoirs is needed, hence TEM and MT resistivity soundings were carried out at the beginning of the 21st century in the valley south of the fjord, where the Laugaland and Botn fields are located. This work presents the methodology and some results from these detailed studies.

2. GEOLOGICAL OVERVIEW OF THE EYJAFJÖRDUR AREA

Eyjafjördur is one of the longest fjords in Iceland with its 70 km. The fjord got its name from the island Hrísey in its central part. The fjords in Iceland were formed during the Quaternary Ice Age, as a result of the outlet of the glacier domes from the middle of the island. The glaciers flooded into the ocean at geographically predefined places, in trenches and valleys (Gudmundsson, 2015). The geology of the Eyjafjördur area has been summarized by e.g. Flóvenz et al., 2010 and Flóvenz and Karlsdóttir, 2000. The geological formations of the study area are mostly tertiary flood basalts with an age around 6 to 9 Ma. These sequences are built up of several layers of tholeiitic lavas, interbedded with scoria and inter-eruptional sediments, olivine tholeiites and porphyric basalts (see details in Figure 1). While the lava piles are deeply glacially eroded, the bedrock at sea level belongs to the mesolite/scolecite alteration zone, the laumontite zone starts at 500 m depth and the epidote zone is at 3000 m depth. The sediment fill in the valley is mostly alluvial. The general dip of the compound lava layers fits well with the trend throughout the whole island, that is the dip points to the rift zone from which the lavas originated, because the bending of the weak crust due to loading of the lava pile. Here this process manifests in a 3-6° dip towards the south, but southwards along the fjord, the dip is to the east. The matrix permeability of the lava formations is negligible, except for the inter-eruptional sediments, so the groundwater flow is fracture-controlled in these formations. However, in the valley fill, the horizontally layered sediments could have some matrix permeability, leading to horizontal groundwater flow. The fractures and faults

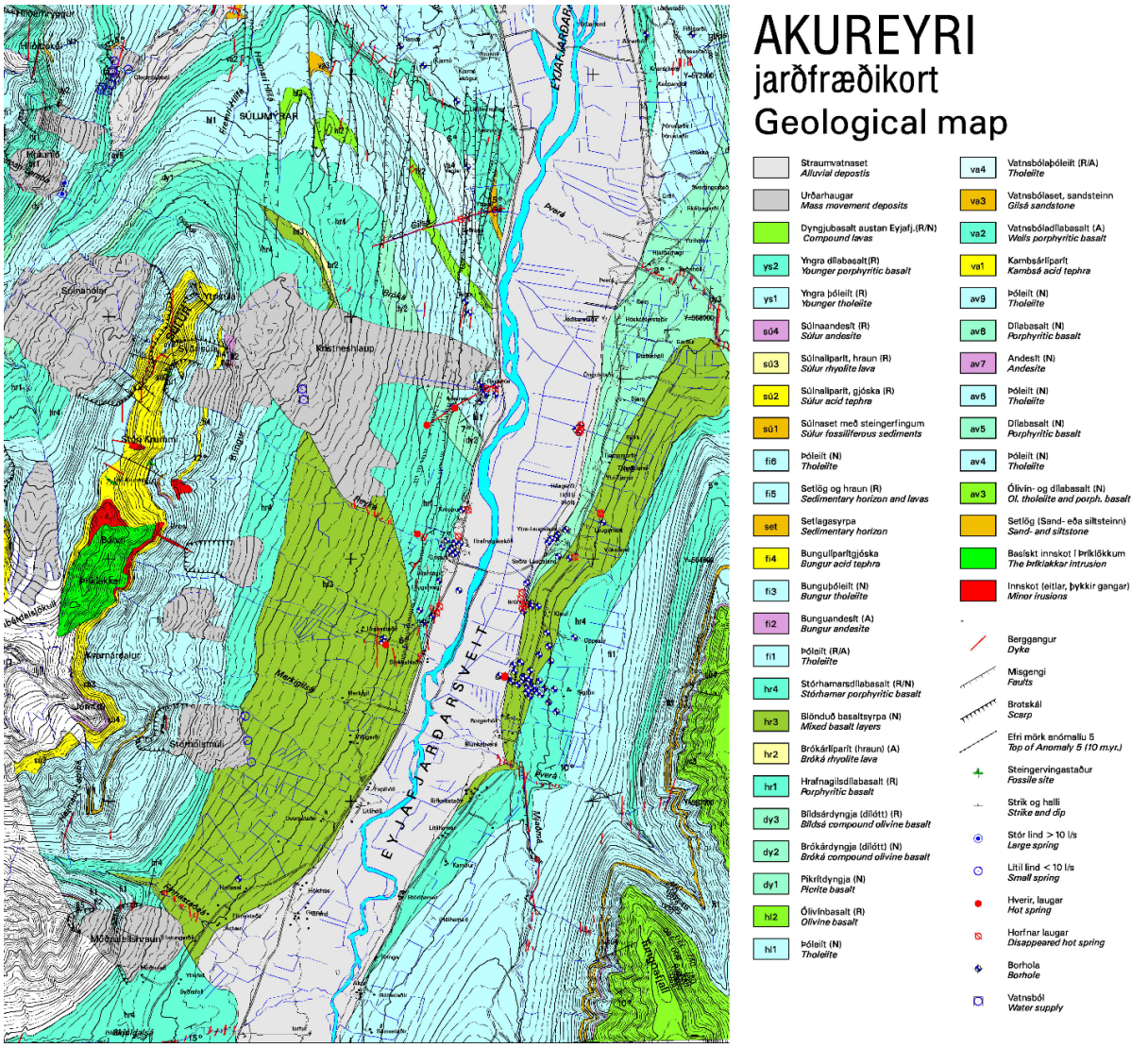

FIGURE 1: Geological map of the Eyjafjördur (Hjartarson and Jónsdóttir, 2004)

are mainly caused by recent tectonic activity at the Tjörnes fracture zone, north of the study area, which is a right lateral transform fault system in the North Atlantic Ocean. The other possible mechanism causing recent tectonic activity might be the glacial isostatic rebound in the area. The geological features in the area that influence ground water flow are near vertical dykes and normal faults. The geothermal temperature gradient in the area is 40-60°C/km which is to be expected as Eyjafjördur is located 100 km west of the active rift zone. Because of the low heat flow the geothermal fields of Eyjafjördur are low-temperature fields with reservoir temperature ranging from 50 to 100°C (Flóvenz and Karlsdóttir, 2000). Within the formations, two heat transfer mechanisms could be present: - heat conduction in the uneroded lava piles and convective cells in the fractures (Flóvenz and Saemundsson, 1993).

3. ELECTROMAGNETIC GEOPHYSICAL METHODS – THEORY AND APPLICATION

Resistivity methods are geophysical methods widely used in geothermal exploration, where the investigated geological formations are distinguished by their electrical properties, because in geothermal fields, the fluid content and the alteration mineralogy can lead to sharp resistivity contrasts compared to the generally resistive rocks. This statement applies especially in fracture-dominated areas like Eyjafjördur, where the convection of the hot fluid gives rise to a low-resistivity anomaly. Early on, the methods applied were based on the injection of direct current into the ground through two electrodes, with the potential field measured between other two electrodes. To reach reasonable penetration depths a few kilometres of cables have to be used. Therefore, this method is fairly slow to use and requires a lot of field work, if reasonable amount of data is to be collected. In addition, at places where the uppermost layer has high resistivity, for example lava fields, it is nearly impossible to inject enough current into the ground, to reach good depth of penetration. The data processing is though relatively easy for these measurements. To overcome these difficulties new techniques were needed. The solution to this was implementation of electromagnetic methods. In Iceland, these methods were implemented in the mid-1980s and proved very successful in geothermal exploration.

The common principle in resistivity sounding methods is to induce currents in the ground and measure the response. In DC methods the electrical field is built up by injecting currents into the ground, while in the case of electromagnetic methods discussed here, the currents in the ground are induced by a time varying magnetic field. This time varying magnetic field could have two types of sources; in the case of naturally varying field we speak about the magnetotelluric method (MT), while if the magnetic field is artificial the method usually referred to is the Transient Electromagnetic Method (TEM). The natural sources of the magnetic field of the MT method are the daily varying ionospheric and magnetospheric currents, with these processes giving low-frequency variation, whereas the high-frequency variations are induced by thunderstorm activity around the equator. Although, this high frequency signal is stronger at low latitudes, it can be measured at higher latitudes too, because the electrical signal created by the thunderstorm, travels as a guided wave between the earth and the ionosphere to higher latitudes. Between the two frequency ranges a band is present where the intensity of the signal is considerably lower, it is called the MT-dead band and ranges from 0.5 to 5 Hz. In contrast with this, the TEM measurements use a controlled source to build up time varying magnetic field created by transmitting current into a loop. When the current is turned off, currents are induced in the ground giving raise to decaying magnetic field which decay rate is measured by induction in a receiver coil.

3.1 Conductivity of rock formations - consequences of the temperature of a geothermal system

The resistivity methods are fundamentally important in geothermal prospecting, because they measure properties of rocks, which are strongly related to the fluid content and temperature of the reservoir. These parameters determine the quality of a geothermal reservoir. Therefore, resistivity methods give valuable information about the reservoir itself. In most rocks in low-temperature areas the main electrical conduction mechanism is the electrolytic conduction in aqueous solutions flow in the pore

space of the rocks, while the rock matrix is an insulator. The electrical resistivity of rocks depends on several factors: porosity and pore structure, water saturation, ion content of the water, temperature, phase of the fluid and the water rock interaction. Although the above mentioned factors determine mainly the resistivity of rocks, different rock types can have different resistivity as shown in Table 1 (Hersir and Björnsson, 1991). Since high-temperature geothermal fields are usually in volcanic areas, the relationship between the formations at these areas and the resistivity structure is fundamental. The resistivity structure in high-temperature geothermal areas is not correlated with the lithology, but with the alteration mineralogy. These altered formations are created by the high-temperature fluid flow in the surrounding rocks. As the substantial majority of the rock formations in Iceland, the compound lavas of Eyjafjördur were formed along the rift system under high-temperature conditions, so these rocks are altered too. A general alteration structure in a high-temperature area starts with the smectite-zeolite zone with resistivity values ranging from 5 to 10 Ωm, below the unaltered rocks. These clay zones act as a low-permeability cap rock of the system. This zone is followed by the high-resistivity core with the chlorite and chlorite-epidote zoning. The grade of the alteration depends primarily on the temperature of the fluid. Therefore, the resistivity structure is a first approximation for the formation temperature. However, this only applies if the geothermal system is in temperature equilibrium. In the case of an old or young system the temperature deduced from the alteration mineralogy can differ from the actual formation temperature (Flóvenz et al., 2012).

TABLE 1: Resistivity of Icelandic rocks (Hersir and Björnsson, 1991)

Formation	Resistivity (Ωm)
Recent lava flows, above groundwater table	5,000-50,000
Dense intrusives (gabbro, dolerite)	10,000-15,000
Recent lava flows, below groundwater table	100-3,000
Basalts, rather dense	100-300
Palagonite	20-100
Low-temperature areas in basalt formation	30-100
Low-temperature areas in hyaloclastite formation	10-50
Rocks with brine	5-15
High-temperature areas, fresh water	1-5
High-temperature areas, brine areas	1-4

3.2 Electromagnetic theory for MT measurements

In this section the basic electromagnetic theory for the magnetotelluric method will be discussed. It is based on the response of the subsurface conductors to incoming waves of time varying magnetic fields. Therefore, Maxwell equations describe the problem:

$$\nabla \times \mathbf{H} = \sigma\mathbf{E} + \varepsilon\frac{\partial \boldsymbol{E}}{\partial t} \tag{1}$$

$$\nabla \times \mathbf{E} = -\frac{\partial \boldsymbol{B}}{\partial t} \tag{2}$$

$$\nabla \cdot \mathbf{B} = 0 \tag{3}$$

$$\nabla \cdot \mathbf{E} = \frac{1}{\varepsilon}\eta \tag{4}$$

where **E** is the electric field in V/m, **H** is the magnetizing field vector in A/m, **B** is the magnetic flux density vector in T, ε is the electrical permittivity in As/Vm, η is the electrical charge density in C/m^3 and the relationship between **H** and **B** is the following: $\mathbf{B} = \mu\mathbf{H}$ where μ is the magnetic permeability.

Considering the assumption, that there is no charge density and after some algebraic transformation, we get the following equations:

$$\nabla^2\mathbf{E} - \mu\sigma\frac{\partial}{\partial t}\mathbf{E} - \mu\varepsilon\frac{\partial^2}{\partial t^2}\mathbf{E} = 0 \tag{5}$$

$$\nabla^2\mathbf{H} - \mu\sigma\frac{\partial}{\partial t}\mathbf{H} - \mu\varepsilon\frac{\partial^2}{\partial t^2}\mathbf{H} = 0 \tag{6}$$

If $\sigma \simeq 0$ (a non-conductive medium) these equations are wave equations, if σ is non-zero these equations are diffusion equations. For the easier discussion it is worth to introduce a vector **A** where the expression is the same for the electric and magnetic field, later it will be used instead of the separate notation of **E** and **H**. If the fields vary harmonically in time (as $e^{i\omega t}$) the following forms can be used:

$$\nabla^2\mathbf{A} + k^2\mathbf{A} = 0 \tag{7}$$

With the complex number, k^2:

$$k^2 = \mu\varepsilon\omega^2 - i\mu\sigma\omega \tag{8}$$

The differential equation (Equation 7) has a plane wave solution. Consider the solution where the wave propagates in the direction of **u**:

$$\mathbf{A}(\boldsymbol{x}, t) = \mathbf{A}^+ e^{-\beta\boldsymbol{u}\cdot\boldsymbol{x}} e^{-i(\alpha\boldsymbol{u}\cdot\boldsymbol{x}-\omega t)} \tag{9}$$

which is a wave propagating with the velocity:

$$v = \frac{\omega}{\alpha} \tag{10}$$

where α and β are equal to the following expressions:

$$\alpha = \sqrt{\epsilon\mu}\omega\sqrt{\frac{1}{2}\left(\sqrt{1+\left(\frac{\sigma}{\varepsilon\omega}\right)^2}+1\right)} \tag{11}$$

$$\beta = \sqrt{\epsilon\mu}\omega\sqrt{\frac{1}{2}\left(\sqrt{1+\left(\frac{\sigma}{\varepsilon\omega}\right)^2}-1\right)} \tag{12}$$

After expressing the components of k and considering the assumption based on the values of the conductivity, the electrical permittivity and the angular frequency, it can be shown that:

$$\frac{\sigma}{\varepsilon\omega} \gg 1 \tag{13}$$

By using this approximation (called the quasi-stationary approximation) in Equations 11 and 12 the following relationship appears for α and β:

$$\alpha \simeq \beta \simeq \sqrt{\frac{\mu\omega\sigma}{2}} \tag{14}$$

Equation 14 can be written as:

$$\frac{1}{\beta} = \delta = \sqrt{\frac{2}{\mu\omega\sigma}} \tag{15}$$

which is the depth where the amplitude has decreased to e^{-1} of its surface value, known as the skin depth (penetration depth).

The penetration depth depends on the frequency of the wave and the conductivity of the medium. Suppose the wave propagates in the direction of **u** with the wave vector **k** = *k***u** from. From Equation 9 we get the following wave equation:

$$\mathbf{A}(\boldsymbol{x}, t) = \mathbf{A_0} e^{-i(\boldsymbol{kx}-\omega t)} \tag{16}$$

From Equations 3 and 4 and from the condition that the charge density is zero, it is seen that:

$$k \cdot \mathbf{E} = k \cdot \mathbf{u} \cdot \mathbf{E} = 0 \tag{17}$$

$$k \cdot \mathbf{H} = k \cdot \mathbf{u} \cdot \mathbf{H} = 0 \tag{18}$$

Therefore, the electrical and magnetic field is perpendicular to the propagation direction. After putting Equation 16 into Equation 1, and changing back **A** to the adequate notation and assuming that **u** is parallel to the z-axis the following expressions add up:

$$E_x = \frac{\mu\omega}{k} H_y \tag{19}$$

$$E_y = -\frac{\mu\omega}{k} H_x \tag{20}$$

Or, in matrix notation:

$$\begin{pmatrix} E_x \\ E_y \end{pmatrix} = \begin{pmatrix} Z_{xx} & Z_{xy} \\ Z_{yx} & Z_{yy} \end{pmatrix} \begin{pmatrix} H_x \\ H_y \end{pmatrix} \tag{21}$$

where the **Z** tensor is the complex impedance tensor, which contains information on the subsurface resistivity distribution.

While the **Z** tensor in Equation 21 is antisymmetric, in case of homogenously layered Earth and a steady-state approximation the resistivity can be expressed as:

$$\rho = \frac{1}{\sigma} = \frac{1}{\mu\omega} \left| \frac{E_x}{H_y} \right|^2 = \frac{1}{\mu\omega} \left| \frac{E_y}{H_x} \right|^2 \tag{22}$$

An additional parameter is calculated, the phase:

$$\theta = \arg(Z) \tag{23}$$

The measured values are the time varying E_x, E_y and H_x H_y and H_z values, of which the apparent resistivity can be calculated depending on the measuring frequency after Kaufman and Keller, 1983.

3.3 Static shift problem

The MT method, as any other resistivity method, where the electric field is measured on the surface is affected by the telluric or static shift problem. It is manifested as an unknown multiplier of the apparent resistivity. This unknown multiplier is independent of frequency, which means the effect of the surface is seen in the long period data reflecting the resistivity structure at great depth. This phenomenon can be caused by near surface resistivity inhomogeneities or significant topography around the station. According to Árnason (2015) two types of near-surface resistivity inhomogeneity exist: 1) electric field distortion due to the dependency of the electric field on the resistivity of the material where the voltage difference is measured and 2) current distortion, when the current is channelled or repelled by a resistivity inhomogeneity. If we consider a section under the measuring site, where a lower resistivity section is surrounded by higher resistivity, the measured electric field in the low resistivity is lower,

giving too low apparent resistivity. Current channelling happens when current is flowing in the ground within a localised resistivity anomaly and the current lines are deflected. If the anomaly has lower resistivity than its environment the current lines are deflected into the anomaly, if the anomaly has higher resistivity the current lines are repelled from it. If the resistivity inhomogeneity is close enough to the surface, this will affect the current density at the surface and hence the electric field and apparent resistivity.

The effect of the topography can also lead to a static shift, manifesting in current distortion. The laterally flowing current density is spread out in the vicinity of local highs but concentrated in topographic lows. Compared with a constant resistive earth, it leads to apparent resistivity lower than the actual resistivity on topographic highs and higher apparent resistivity in topographic lows. Because these processes affect our results the amount of the static shift has to be determined. The solution is brought by Transient ElectroMagnetic measurements - TEM, which is affected only at early times by the above mentioned phenomena. The resistivity values calculated from the late times are comparable to the values measured by MT at the same periods. Hence the ratio between the two values give the value of the static shift multiplier and this value can be used to correct the whole resistivity curve measured by MT, since the shift multiplier is independent of the frequency.

3.4 Magnetotelluric and Transient ElectroMagnetic data collection

In both methods time varying potential fields are measured, so the recorded data are time series data. Since for the MT method long wavelength information is needed, the data collection takes usually about one day. For TEM the data collection is much shorter, so the instrument is not left in the field for one day, as the data collection only takes a few tens of minutes. In the following section, the data collection process for each method will be discussed.

A typical MT sounding station is shown in Figure 2. In pursuance of MT measurements five channels are recorded. Two perpendicular electrical components parallel to the surface are measured by electrodes and three magnetic components in orthogonal directions are measured by magnetic coils. The direction of the setup is aimed to the magnetic north direction, such that the E_x component points to the magnetic north, and the E_y component is in the magnetic east direction. The two horizontal magnetic coils are parallel to the electrical directions, and the third component is the vertical component of the magnetic field measured perpendicular to the surface. The dipole length between the electrodes is usually 50 m. A remote reference station is set up with only the surface-parallel magnetic coils far from any cultural noise and far from the measuring station in order to decrease the noise in the dataset. This is done so the uncorrelated noise can be extracted from the dataset. There are several practical ways to reduce the noise in the measured data; for better contact with the ground, bentonite and water is applied in the holes where the electrodes are put into, in order to increase the contact with the Earth. As with seismic data collections, the wind noise can be seen in the dataset, small currents are induced in any of the long cables by the wind, which makes the dataset noisy. Therefore, these cables should be covered.

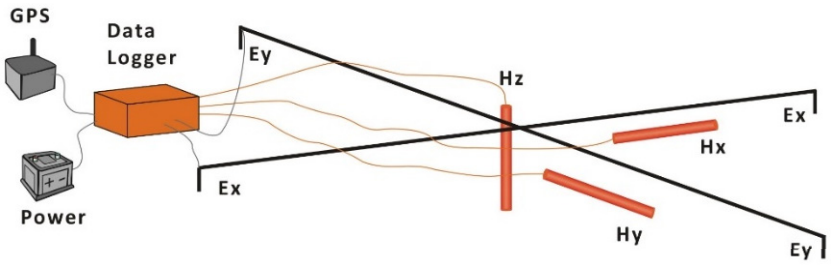

FIGURE 2: A typical layout of an MT measurement (Flóvenz et al., 2012)

In the case of central-loop TEM measurements, loops are applied to measure and to induce electrical field in the ground. Each coil is laid down around the centre of the station, the bigger loop is the source, usually a rectangular loop with the effective area around 40,000 m^2, while the receiver loops are smaller

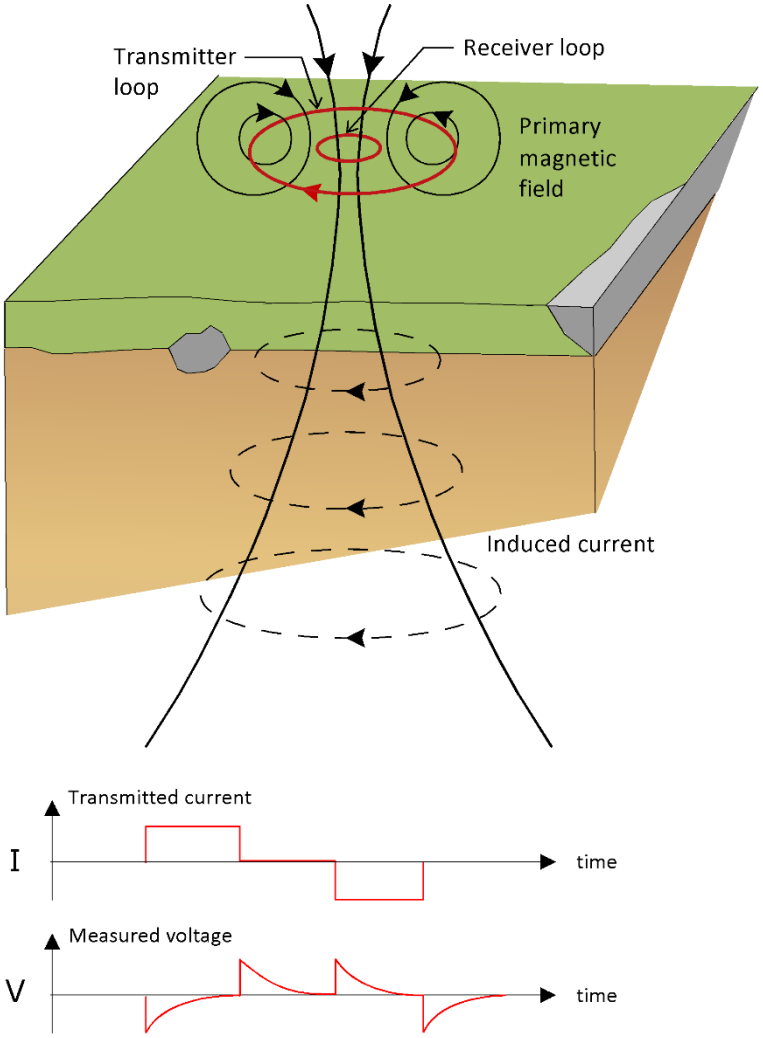

FIGURE 3: Typical layout of a TEM measurement (Flóvenz et al., 2012)

ones with the effective area about 100 m^2 and 5,700 m^2 in the centre of the source loop. The current frequency varies for the different receiver loop, it is either 2.5 Hz or 25 Hz. Into the source loop, a half-duty square wave is transmitted, after turning off the current in the source loop, the decay rate of the magnetic field is measured in the receiver coil, by recording the induced voltage in the receiver loop. As it is impossible to turn of the voltage instantaneously the transmitters turn off the current linearly during a short but finite time, the so called turn-off time. Therefore, the measurements are done in the receiver loop according to the time when the current in the source loop becomes zero. It means that the receiver has to know the turn-off time. In order to reduce the electro-magnetic noise in the signal, the recorded transients are stacked over a number of cycles before storing. The depth of penetration depends on the time after the current is turned off, the longer the elapsed time, the deeper the penetration depth. The resulting dataset consists of voltages at the time gates for the selected frequency, selected gain and the effective area of the receiver loop (Árnason, 2006a). The schematic layout and the transmitted and induced current curves of a TEM sounding are shown in Figure 3.

A complete discussion of the central loop TEM problem is not the purpose of this work, only the forward problem is shown here. The complete discussion of the central-loop TEM problem can be found in Árnason (1989). The induced voltage *V(t,r)* for a central loop configuration in a homogenous half space is given by the following expression:

$$V(t,r) = I_0 \cdot \frac{C(\mu_0 \sigma r^2)^{2/3}}{10\pi^{1/2} t^{5/2}} \tag{24}$$

where *C*:

$$C = A_r n_r A_s n_s \frac{\mu_0}{2\pi r^3} \tag{25}$$

is a constant, containing the properties of the coils, *A* is the areas for the receiver and source loops, respectively, and *n* is the number of turns in the coils. In Equation 24, I_0 is the current in the source loop, μ_0 is the magnetic permeability in vacuum in H/m, σ is the conductivity of the media in S/m, *r* is the radius of transmitter loop, *t* is the elapsed time after the transmitter current is turned off.

Equation 24 is used as the forward problem in the TEM inversion. However, from this equation the apparent resistivity is expressible, as the following relationship:

$$\rho_a = \frac{\mu_0}{4\pi}\left(\frac{2\mu_0 I_0 A_r n_r A_s n_s}{5t^{5/2}V(t,r)}\right)^{2/3} \tag{26}$$

3.5 Joint interpretation of TEM and MT resistivity soundings

3.5.1 TEM and MT data processing

The outputs of an MT measurement are time series data of the three components of the magnetic field and the two components of the electrical field. The processing of the dataset is done in a software developed by Phoenix Geophysics. The first step is to make sure that the five different components and the remote reference station are synchronized so the further processing uses the appropriate dataset. It is done via editing the table files, from which the program reads out the proper association of the data. When it is done the next step is to define the processing parameters for the Fourier transformation. The data are in the time domain but in Equation 22 the data must be in the frequency domain, therefore the Fourier transformation is a crucial step during the processing. For each frequency value there are 5 different corresponding magnetic and electrical values, from which the apparent resistivity and the phase (from Equation 23) can be calculated. The next step is the graphical editing of the apparent resistivity and phase curves in the MTeditor program, from Phoenix Geophysics. Next, the results of the processing are exported as edi files. The last step is converting these files into a Unix compatible format, which is the input for the inversion. An example of the result of the MT processing is shown in Figure 4.

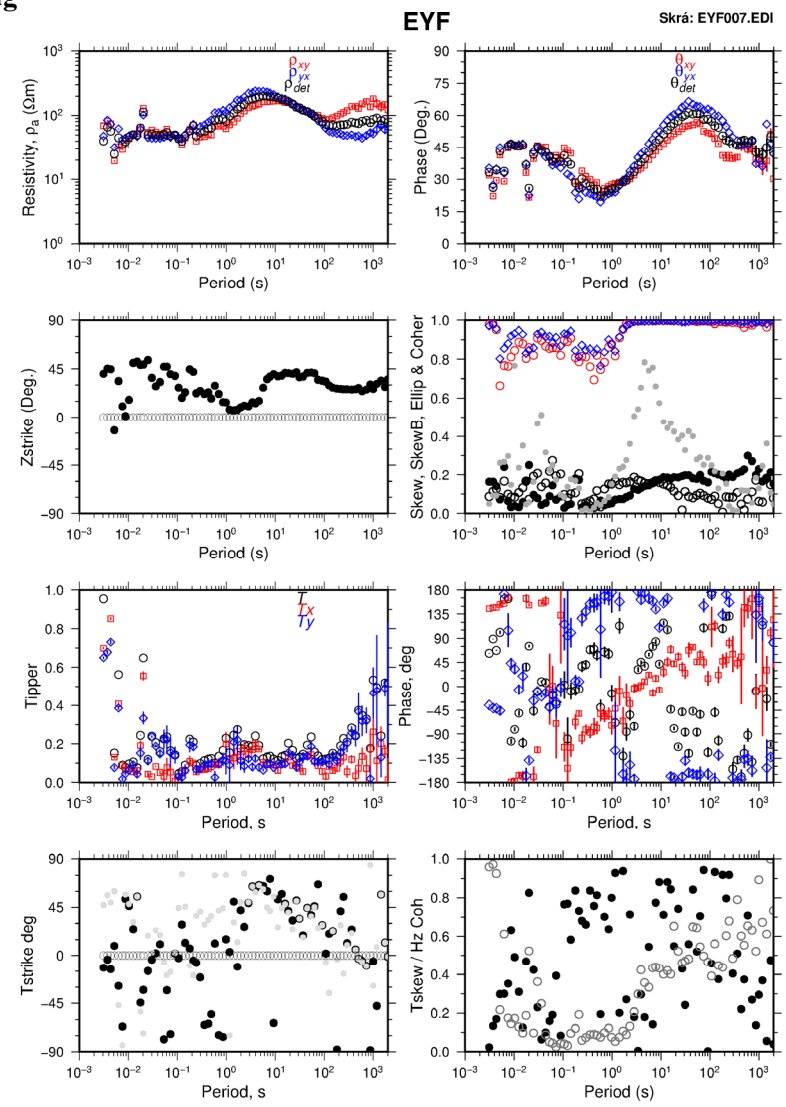

FIGURE 4: On the upper left panel the resistivity values are plotted, as a function of period in both directions as well as the resistivity value calculated from the determinant of the impedance tensor. On the top right panel the three associated phases are plotted. On the other panels additional parameters are plotted, which will not be discussed in detail. It has to be remarked that in the coherency plot (blue and red circles in the second uppermost right panel) the MT dead band appears as a low coherency

For the processing of the TEM data a Unix based software is used, which was developed by Knútur Árnason at ÍSOR (Árnason, 2006a). In

this program, through a graphical interface, the data are edited, so the outliers are omitted and the parts of the apparent resistivity curves, which were measured with different current frequencies are linked. The resulting file contains apparent resistivity values as a function of time after current turn off.

3.5.2 Joint inversion of MT and TEM data

Because, both methods have their limitation, a joint interpretation of the datasets is necessary in order to get the best results. As the MT measurement are affected by the above discussed static shift problem, the measurements have to be corrected by adjusting them to the TEM measurements, which are not affected by the static shift. However, the TEM cannot be used by itself because it has limited depth of penetration depending on the parameters of the loop. The inversion process is made in two steps: at first MT measurements are inverted with a constant resistivity model as the starting model. The output of this inversion is the starting model for the joint inversion, where the static shift is calculated. For the inversion, Occam (minimum structure) inversion was used. An Occam model is built up of many equally thick layers on a logarithmic scale. The inversion software is also Unix based and called TEMTD, it was developed by Knútur Árnason in 2006 at ÍSOR (Árnason, 2006b). In the appendices report (Kovács, 2016), the results of the TEM and MT processing for all the soundings, the joint 1D inversion for all the sounding pairs as well as all the resistivity cross-sections and depth slices are show.

4. THE TEM AND MT DATASET FROM THE EYJAFJÖRDUR AREA – RESULTS

The following topographical map (Figure 5) shows the location of the TEM and MT stations in the vicinity of the main southern geothermal fields of the Eyjafjördur area. The map also contains the

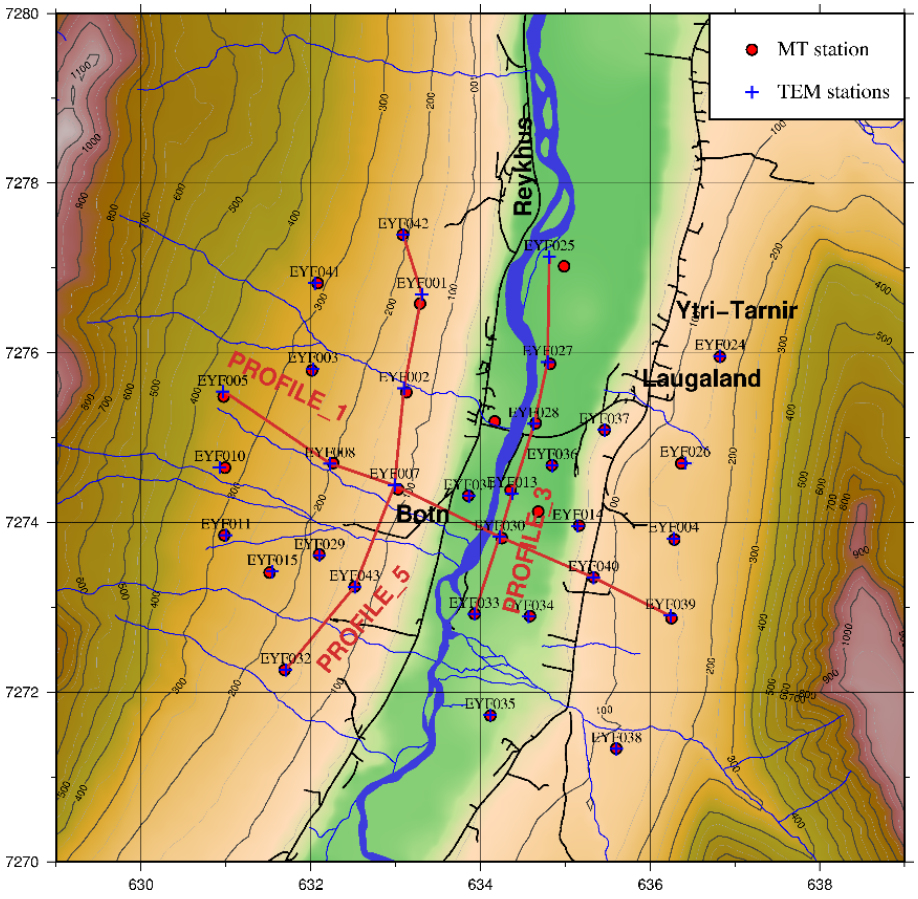

FIGURE 5: Topographical map of the survey area with stations locations; the profiles are shown as red lines

location of the resistivity cross-sections presented. Since the N-S geometry of the valley fundamentally determines the expected resistivity pattern, the orientation of the cross-sections was chosen to be parallel and perpendicular to this main direction. The location of the stations extends from the western part of the valley to the eastern part, covering the bottom of the valley. This dataset extends to the south from the older dataset from the seventies, which was the basis of the discovery of the Laugaland field. The station network covers the Botn field completely, which enables the possibility to compare the results from this study to the work of Flóvenz and Karlsdóttir (2000). During the inversion of the data it was observed that the stations from the valley (EYF027 station in Figure 6) gave much higher misfit than those situated on the mountainside (EYF043 station in Figure 6). This phenomenon was due to the great resistivity variation of the shallow part. Certainly, the uppermost high-resistivity layer is the part which is above the water table, the low-resistivity part is the water saturated sediments and the following high-resistivity part is the bedrock of the valley. It is fundamentally important to distinguish these two types of soundings, because of the flat and horizontally layered geometrical assumption in the inversion. The TEM soundings over conductive sediments see the flanking resistive bedrock of the valley, and cannot be fitted by horizontally-layered model. An example is shown in Figure 6 for both resistivity structures.

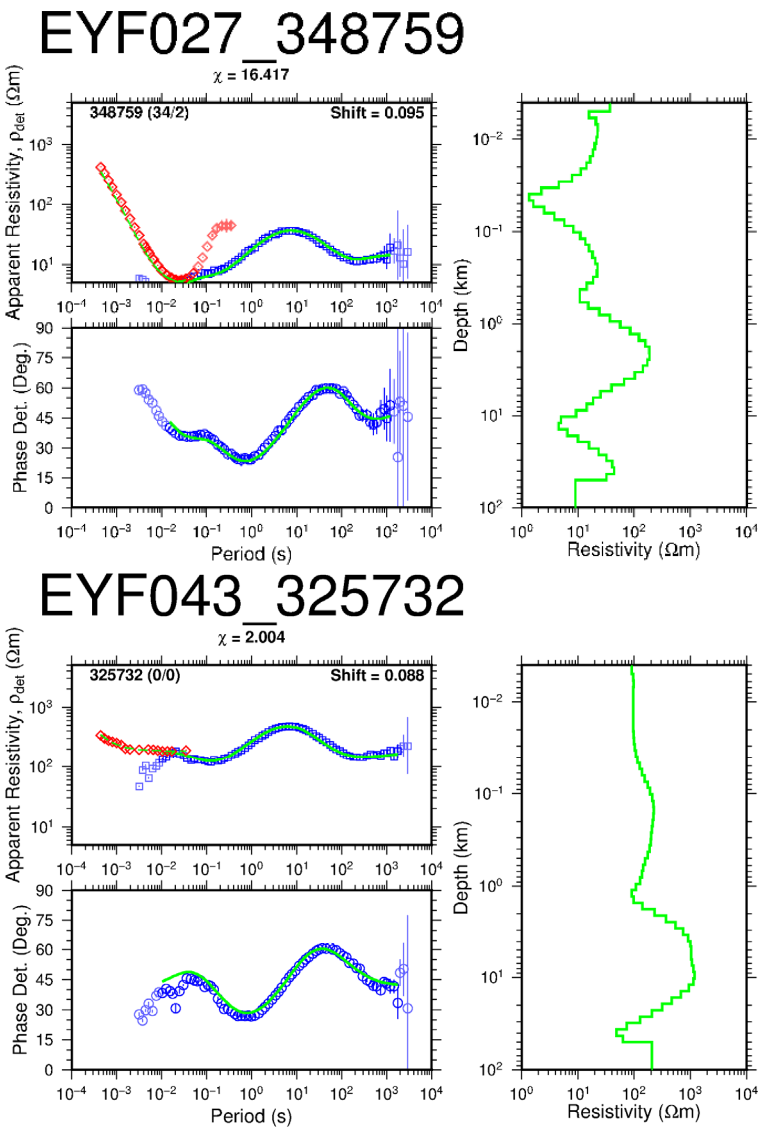

FIGURE 6: On the upper left panels the red dots show the measured apparent resistivity from the TEM data, the blue dots show the measured apparent resistivity from the MT data, the lower left panel shows the measured phase. On the right panel the calculated Occam resistivity is plotted. The green curve on the left side panels is the calculated response of the model

5. INTERPRETATION

It is known from the results of Flóvenz and Karlsdóttir (2000) that the Botn field is a fracture-controlled geothermal system, where the strike of the fault is NE-SW, as is expected from the orientation of the valley. In the above-mentioned work, the authors reached the conclusion that this fracture is sealed by secondary mineralization, which acts as an aquifuge. A permeable layer conducts the water flow to the north where it ascends to the surface along dikes and fractures as shown in the N-S cross-section in Figure 7 from the same work. In Figure 8 the resistivity image of the southernmost 5 km of the resistivity model is shown.

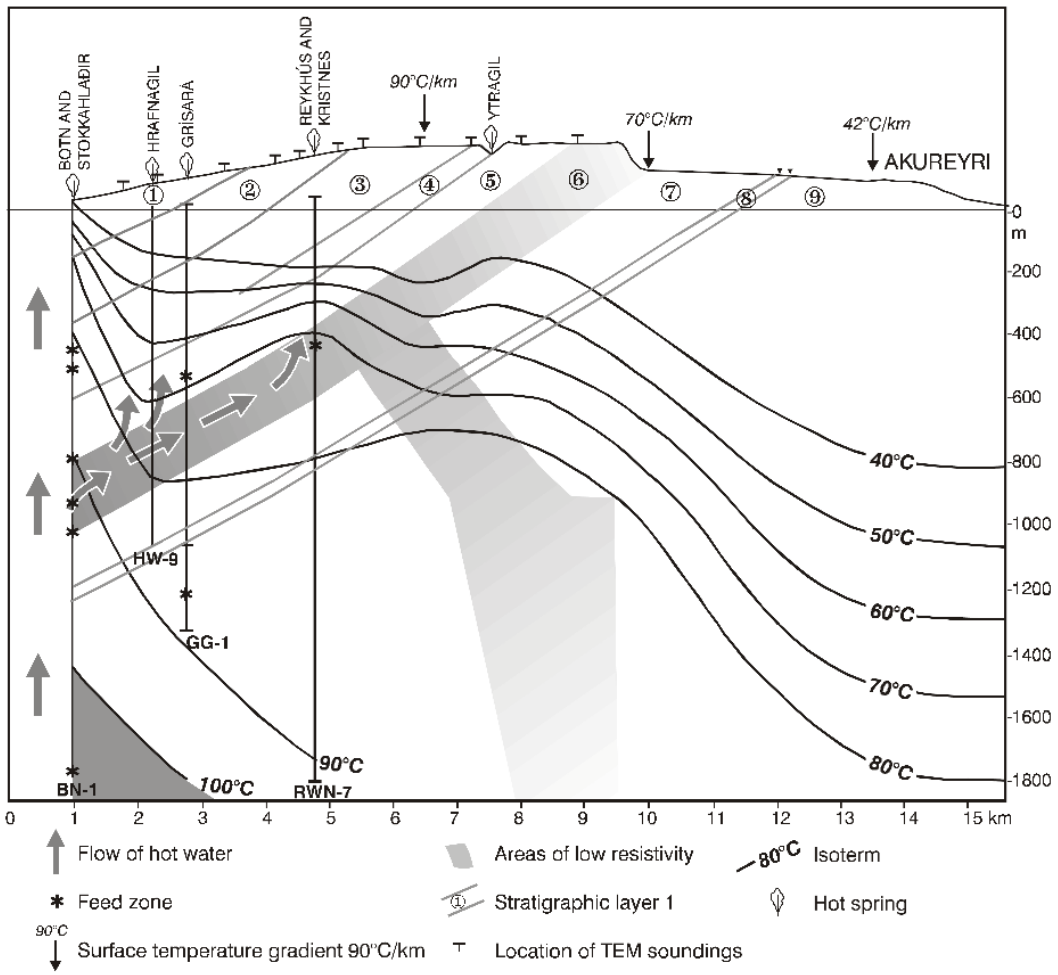

FIGURE 7: Conceptual model of the Botn field (Flóvenz and Karlsdóttir, 2000)

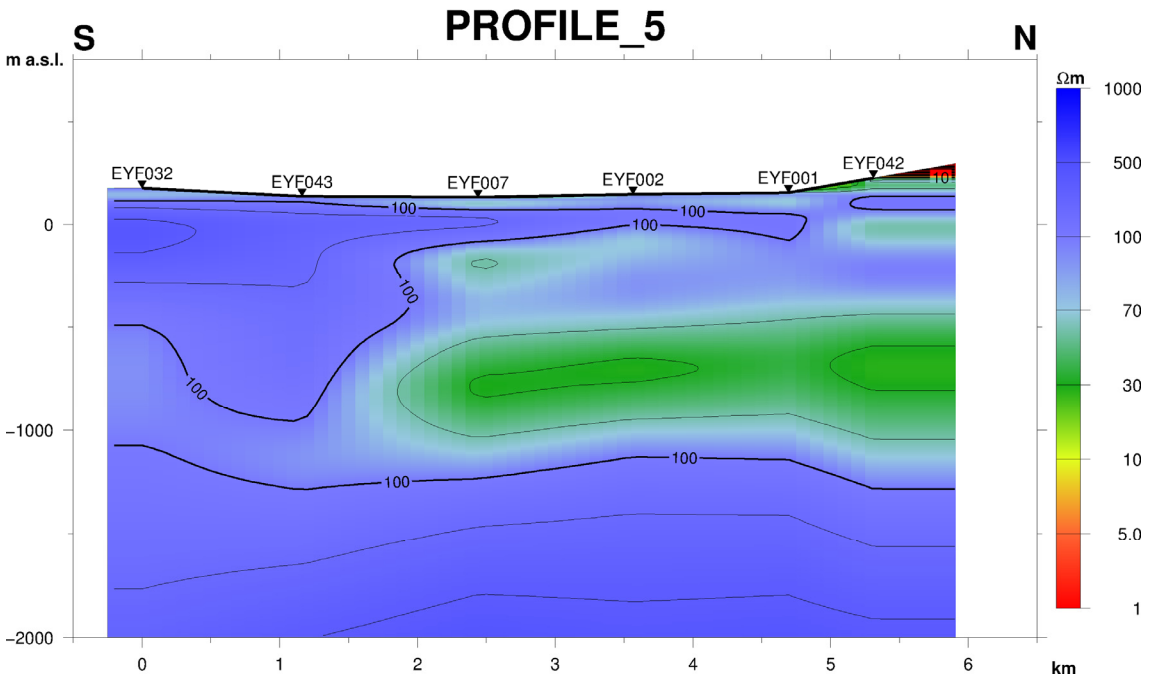

FIGURE 8: Resistivity profile showing the southernmost part of the conceptual model from Flóvenz and Karlsdóttir (2000); black triangles show the location of the MT soundings; location of the profile is given in Figure 5

It is apparent that a near-horizontal low-resistivity layer is mapped pretty well, at around 1 km in Profile_5. This corresponds to the southernmost 5 km of the dipping water flow discussed in the above mentioned work. However, the ascending part of the water-flow was not mapped by this resistivity survey, but it is probably along a near-vertical dike or fault. It is seen clearly on the resistivity depth slices in Appendix V (Kovács, 2016), that this anomaly extends further to the east. According to the resistivity structure in Profile_5, and in order to understand better the behaviour of the reservoir, a perpendicular cross-section was drawn, which crosses the valley itself (Figure 9). The low-resistivity anomaly on this cross-section shows the extent of the field in the valley. However, the resistivity structure is very similar to the concluded resistivity distribution in Flóvenz et al. (1985), for Quaternary formations. It is the author's opinion, that this low-resistivity anomaly is the same structure as discovered in the seventies, leading to the discovery of the deep Laugaland system (Flóvenz et al., 2010).

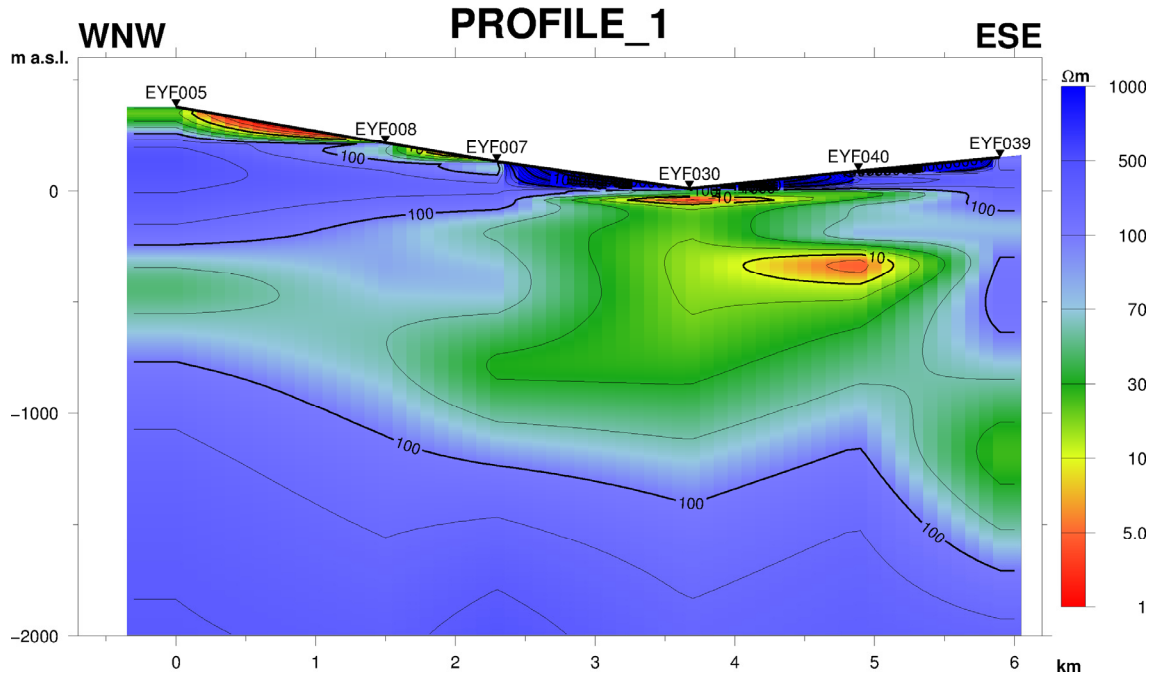

FIGURE 9: The shallow valley crossing resistivity profile; black triangles show the location of the MT soundings; location of the profile is given in Figure 5

For the proper usage of a geothermal field, it is necessary to understand the whole system, with its key elements such as its geometrical characteristics and of course the heat source. Therefore, a deeper version of Profile_1 is presented in Figure 10. In this cross-section, a pronounced low-resistivity anomaly is seen from 7 km depth down to the bottom of the plot. It is also seen in the deeper lying depth slices in Appendix V (Kovács, 2016) that this low-resistivity anomaly extends further down, its direction, coinciding with the direction of the valley. It raises the question, what is the cause of such a deep-seated low-resistivity anomaly. It cannot be a huge fluid saturated reservoir at such a depth, because pore spaces and fractures are mostly closed under high lithostatic pressure. Also, it cannot be a highly altered zone, because the highly altered formations are not far away from the surface, due to glacial erosion. Hersir et al. (1984) described such a deep-seated, low-resistivity anomaly, where they suggested, that the low-resistivity anomaly was caused by enrichment in basaltic melt, which has lower resistivity than ultramafic rocks. This deep-seated enigmatic low-resistivity anomaly is seen below most of Iceland, based on data from numerous surveys. If it was a partially melted body, then these anomalies should cause seismic S-wave attenuation, although these anomalies are not seen. Árnason et al. (2010) proposed similar resistivity anomalies based on data in the Hengill area, which might reflect sheeted dike complex. These basaltic dikes and intrusions are ductile, while the underlying gabbro formations are more brittle. It is known from a recent structural geological study (Proett, 2015), that the deformation styles show sinistral strike-slip and normal faulting in the area. As a result of the normal faulting and

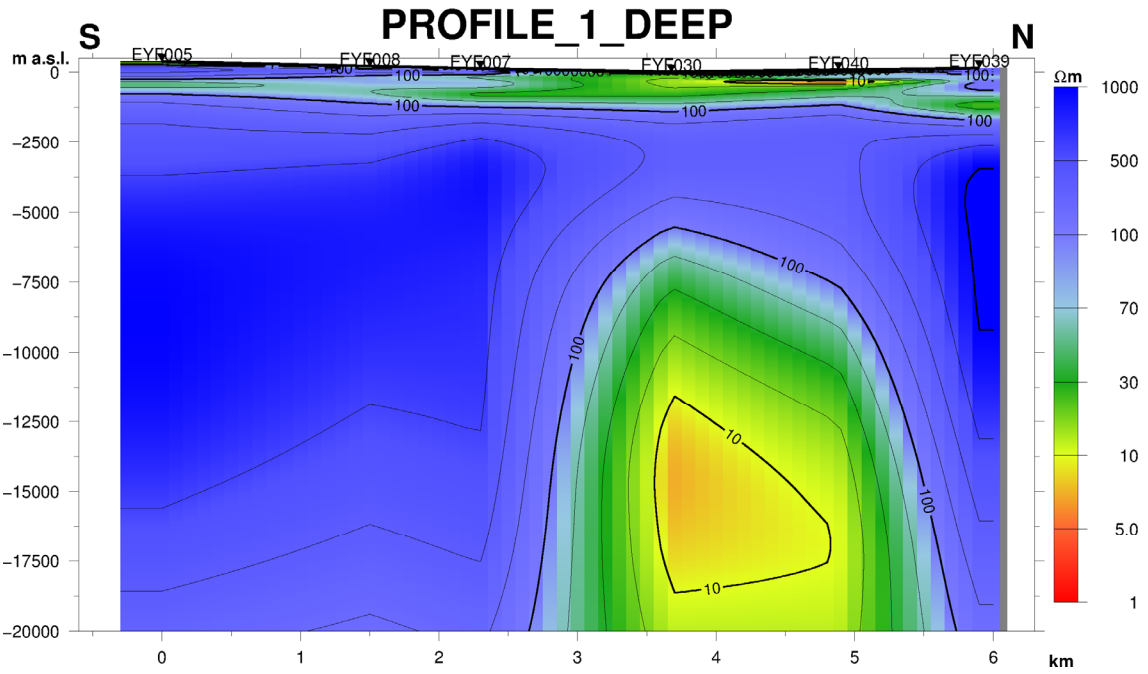

FIGURE 10: The deep valley crossing profile; black triangles show the location of the MT soundings: the location of the profile is given in Figure 5

the extensional component of the sinistral strike-slip faulting, a space could be developed, where the intrusives could be pushed into.

6. DISCUSSION

In this study the methodology of the electromagnetic method was described, concentrating on the Magnetotelluric method (MT) and the Transient Electromagnetic method (TEM). A dataset from Eyjafjördur was processed and interpreted. As a result, the low-resistivity anomaly caused by warm groundwater flow was confirmed from former studies. A proposal for the interpretation was made for an enigmatic and highly debated resistivity structure.

The methods discussed here seem to be a powerful tool to detect shallow resistivity structures, which coincide with formerly confirmed geothermal reservoirs. The MT method can be used to detect deep seated inhomogeneities, although it cannot give a clear picture of these formations on its own. Therefore, further studies are required in order to understand the described phenomena.

ACKNOWLEDGEMENTS

I would like to thank Mr. Lúdvík S. Georgsson and his colleagues for their devoted work, which resulted as an unforgettable and immensely precious six months. A special thank must be said to Mr. Gylfi Páll Hersir for showing me the geophysical methods, which are used successfully in geothermal research. I thank Mr. Knútur Árnason for showing me the example of how a physicist could contribute in geophysical work, and of course I must thank him for introducing me to the new world of Unix. I have to thank Ms. Ásdís Benediktsdóttir for her always helping advices. And naturally all UNU fellows, who showed me a beautiful world through their personality. Nordurorka is acknowledged for allowing the use of the resistivity data from the Eyjafjördur area for this project.

And I must say thanks to my family who helped me to get into this nice profession, with their suggestions and the stable base. I must say thanks to my girlfriend who helped me get through the lonesome moments during last year. And my beloved grandfather, whom I lost during this period, köszönöm Papa.

REFERENCES

Árnason, K., 1989: *Central loop transient electromagnetic sounding over a horizontally layered earth.* Orkustofnun, Reykjavík, report OS-89032/JHD-06, 129 pp.

Árnason, K., 2006a: *TemX, a graphically interactive program for processing central-loop TEM data – A short manual.* ÍSOR – Iceland GeoSurvey, Reykjavík, internal report, 17 pp.

Árnason, K., 2006b: *TEMTD, a programme for 1D inversion of central-loop TEM and MT data – A short manual.* ÍSOR – Iceland GeoSurvey, Reykjavík, short manual, 16 pp.

Árnason, K., 2015: The static shift problem in MT soundings. *Proceedings of the World Geothermal Conference 2015, Melbourne, Australia,* 12 pp.

Árnason, K., Eysteinsson, H. and Hersir, G.P., 2010: Joint 1D inversion of TEM and MT data and 3D inversion of MT data in the Hengill area, SW Iceland. *Geothermics, 39,* 13-34.

Flóvenz, Ó.G., Árnason, F., Gautason, B., Axelsson, G., Egilson, T., Steindórsson, S.H., and Gunnarsson, H.S., 2010: Geothermal district heating in Eyjafjördur, N-Iceland: Eighty years of problems, solutions and success. *Proceedings of the World Geothermal Conference 2010, Bali, Indonesia,* 8 pp.

Flóvenz, Ó.G., Georgsson, L.S., and Árnason, K., 1985: Resistivity structure of the upper crust in Iceland. *J. Geophysical Research, 90-B12,* 10,136-10,150.

Flóvenz, Ó.G., Hersir, G.P., Saemundsson, K., Ármannsson, H., and Fridriksson, Th., 2012: Geothermal energy exploration techniques. In: Sayigh, A. (ed.), *Comprehensive Renewable Energy,* 7. Elsevier, Oxford, UK, 51-95.

Flóvenz, Ó.G., and Karlsdóttir R., 2000: TEM-resistivity image of a geothermal field in N-Iceland and the relation of the resistivity with lithology and temperature. *Proceedings of the World Geothermal Conference 2000, Kyushu – Tohoku, Japan,* 1127-1132.

Flóvenz, Ó.G., and Saemundsson, K., 1993*: Heat flow and geothermal processes in Iceland. Tectonophysics, 225,* 123-138.

Gudmundsson, A.T., 2015: *Living earth – outline of the geology of Iceland.* Mál og menning, Reykjavík, 260-263.

Hersir, G.P., and Björnsson, A., 1991: *Geophysical exploration for geothermal resources principles and application.* UNU-GTP, Iceland, Report 15, 94 pp.

Hersir, G.P., Björnsson, A., and Pedersen, L.B., 1984: Magnetotelluric survey across the active spreading zone in southwest Iceland. *J. Volcanology & Geothermal Research, 20,* 253-265.

Hjartarson, Á., and Jónsdóttir, H.E., 2004: *Akureyri, geological map* (2nd ed.). ÍSOR – Iceland GeoSurvey, Reykjavík.

Kaufman, A., and Keller, G.V., 1983: *Frequency and transient sounding. Methods in geochemistry and geophysics, vol. 16.* Elsevier Scientific Publishing Co., Amsterdam, the Netherlands, 685 pp.

Kovács, A., 2016: *Appendices to the report "Electromagnetic exploration of the Eyjafjördur low-temperature geothermal area".* UNU-GTP, Iceland, report 23 appendices, 72 pp.

Proett, J.A., 2015: *Enigmatic rift-parallel, strike-slip faults around Eyjafjördur, Northern Iceland.* Syracuse University, surface, MSc thesis, 57 pp.